Nano Carbons 2024; 2(1): 234.
Original Research Article

Numerical analysis of discs based on carbon-nanofiber/$Al_2O_3ZrO_2$ nanocomposite materials

Hüseyin Fırat Kayiran

ARDSI Mersin Provincial Coordination Unit, Mersin 33140, Turkey; huseyinfirat.kayiran@tkdk.gov.tr

ARTICLE INFO

Received: 18 September 2023
Accepted: 3 November 2023
Available online: 6 December 2023

doi: 10.59400/n-c.v2i1.234

ABSTRACT: In this study, the behavior of three different discs consisting of AS4 carbon fiber, T-300 carbon, and $Al_2O_3ZrO_2$ (nanocomposite) materials at constant temperature was investigated by the numerical analysis method. Nanocomposites are formed by the dispersion of nanometer-sized particles in a matrix. With the advantages that nanocomposites bring to the material, they increase heat resistance in general. Carbon fibers, on the other hand, are preferred in the aerospace and aircraft industries due to their high strength properties. In this study, it was assumed that the modulus of elasticity does not change with temperature. The temperatures applied to the discs are 45 °C, 60 °C, 75 °C, 90 °C, and 105 °C, respectively. It has been observed that the radial and tangential stress values obtained at high temperatures are higher than at low temperatures. The $Al_2O_3ZrO_2$ nanocomposite materials have found that the stresses occurring in the $Al_2O_3ZrO_2$ (nanocomposite) disc are higher than the stresses occurring in the AS4 carbon fiber disc. The stresses obtained on the AS4 carbon fiber disc are T-300 carbon discs.

KEYWORDS: $Al_2O_3ZrO_2$ (nanocomposite); AS4 carbon fiber; T-300 carbon; elastic stress analysis

1. Introduction

Discs are very important for machine parts. Recently, knowledge of the tensile behavior of discs made of different materials has been considered indispensable for high-temperature machines. Discs have many practical engineering applications, such as in reciprocating and centrifugal compressors, gas and steam turbine rotors, internal combustion engines and turbojet engines, and fly wheels. A brake disc can be an example of a solid rotating disc where only body force is involved. Solid discs can also be found in components such as cover plates for rotating components and idlers used in belt assemblies[1,2]. The thermal analysis of discs is an important issue because of their many practical applications in mechanical engineering.

As an example, in a study conducted, the thermoelastic stresses of rotating discs of variable thickness were investigated. A correlation has been established between thickness and stress[3]. Thermal analysis is a primordial stage in the study of brake systems because the temperature determines the thermomechanical behavior of the structure[4]. Composite materials are used in various fields because they have a long service life, high strength, and low weight. In general, they have recently been preferred in the aviation industry. Carbon fibers, on the other hand, are resistant to corrosion in aviation. In addition, their sensitivity is low despite fatigue cracking[5–7]. The studies conducted in the literature on the production and characterization of alumina-zirconia and other nanocomposite laminates are quite

limited. Some recent studies published in the literature reveal some of the results obtained for composite ceramic laminates[8,9]. When different studies are examined, it is understood that the zircon-reinforced nanocomposite shows high strength compared to other materials[10].

In the other study, steel dampers on a wall panel consisting of square-section frames subjected to a hot rolling process were examined by numerical analysis. The data obtained at the end of the study were processed in the literature. In addition, it has emerged as a result that elastic stiffness is formed at an optimal level[11]. The stresses occurring at different angles of different shock absorbers, accompanied by different temperatures, were studied. At the end of the study, it was found that there is a relationship between temperature and sample strength[12]. In different studies, the elastic angular velocities occurring in the annular disc have been determined. In addition, the results obtained at the end of elastic analyses on rotating circular discs with different properties have been shared with the literature with graphs[13,14].

In another study, the thermomechanical properties of a functionally rated mounted uniform disc with a rigid body/without a body were investigated. The results obtained were compared with each other[15]. In the other study, the estimation of the bending and out-of-plane loading effects on the formability response of steel plates was examined. The results obtained are considered to reveal good results for the literature[16]. The materials used in this study are of vital importance. For example, carbon nanofiber shows the continuous, high strength found in filament counting shots. The material is processed as a high-tensile, PAN-based fiber[17]. Nanocarbon fibers are used in areas requiring high strength; they have different sizes in different forms[18]. Carbon-Nanofiber/$Al_2O_3ZrO_2$ Nanocomposite Materials: $Al_2O_3ZrO_2$ Nanocomposite Material materials are used as catalysts or catalyst supports, oxygen sensors, solid electrolytes, membranes, and high-temperature thermal insulation[19,20]. Alumina (Al_2O_3) is an exceptional ceramic structure known for its unique optical, mechanical, and electrical properties. The strength of Al_2O_3 and Al_2O_3-based ceramics can be enhanced by the application of strategic techniques that may include the inclusion of secondary phase particles (such as zirconia and ZrO_2)[21]. T-300 carbons: carbon fiber can be preferred, especially in the bumper parts of ultra-luxury vehicles. Carbon fiber is the most suitable material for weight reduction studies[22,23].

This study is a numerical study, and the mechanical properties of carbon nanofiber/$Al_2O_3ZrO_2$ nanocomposite materials have been processed in a computer program developed only through mathematical modeling. The results obtained were found to be compatible with the literature. In general, to give information about the production method of nanocomposites and the distribution of reinforced materials to the matrix in an experiment that can be performed at later stages, the need of human society to build low-weight, high-strength, and durable structures has increased the demand for composite materials. In a different study, the effects of carbon nanotubes on the thermal behavior of epoxy resin composites were investigated.

At the end of the study, it was shown that the thermal stability of epoxy composites is directly related to the increase in the percentage of CNTs, as the CNT content increases to 75.0% by weight and the thermal decomposition temperature of epoxy composites increases by 75 °C. In addition, it has been observed that energy absorption increases by 6.0% in CNTs, with an increase of up to 14.4% by weight[24]. In a different study, carbon nanotube-reinforced composite honeycomb sandwich panels were made using silicone molding. During the study, different amounts of nanotubes were added to the epoxy resin to determine the role of carbon nanotubes on the pressure and bending behavior of sandwich panels. The results reveal the conclusion that the compressive strength of honeycomb panels has a direct relationship with the increase in the percentage of carbon nanotubes and the thickness of the wall. For example, when

the compressive strength of sandwich panels increases from 42 MPa to 54 MPa, carbon nanotubes increase from 0.025% to 0.075% by weight[25].

In addition to all these and some other studies conducted in the literature[26–28], there are still visible problems in this area, and more research is needed, so in this study, thermal elastic stress analysis was performed under constant temperature.

2. Material and method

In this study, thermal elastic stresses occurring at temperatures of 45 °C, 60 °C, 75 °C, 90 °C, 105 °C were determined (**Figure 1**).

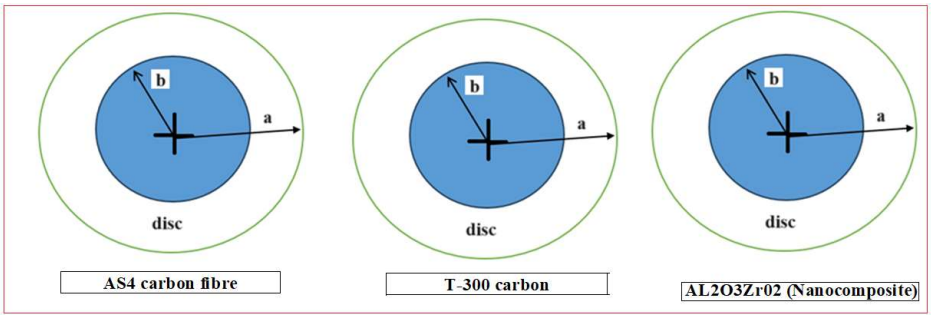

Figure 1. Discs exposed to elastic stress.

Analytical solution

For the composite thin disc, reference can be made to the fact that the plane stress state prevails, i.e., the stresses perpendicular to the plane do not act. σ_r and σ_θ are coefficients of radial and tangential thermal expansion. It shows the constants of the $a_{\theta\theta}$ a_{rr} heavy-elasticity matrix. Here, the expressions of elasticity constants in terms of engineering constants are as follows[29]. **Figure 2** shows the modeled disc subjected to thermal stress.

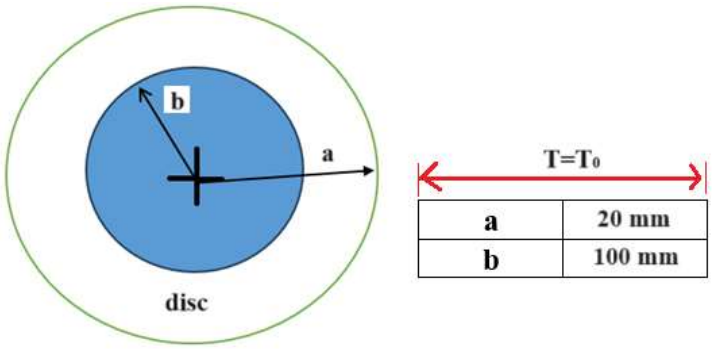

Figure 2. A disc consisting of different materials subjected to thermal stress analysis.

$$a_{\theta\theta} = \frac{1}{E_\theta} \tag{1}$$

$$a_{rr} = \frac{1}{E_r} \tag{2}$$

$$a_{r\theta} = \frac{-\upsilon_{r\theta}}{E_r} \tag{3}$$

Equilibrium equation for plane stress case,

$$\frac{r(d\sigma_r)}{dr} + (\sigma_r) - (\sigma_\theta) + R = 0 \tag{4}$$

It is given in the form. If the mass force R is neglected,

$$k^2 = \frac{a_{rr}}{a_{\theta\theta}} \tag{5}$$

For the general equilibrium equation[29] in the form. The equilibrium equation in which the stress function can be defined as F is as follows:

$$r^2F'' + rF' - k^2F = \frac{(\alpha_r - \alpha_\theta)T}{a_{\theta\theta}}r - \frac{a_{\theta\theta}T'}{a_{\theta\theta}}r^2 \tag{6}$$

r is the radius of the disc at any point, σ_r is the radial stress, and σ_θ is the tangential stress. Change of variables $r = e^t$ can be made. For constant temperature, it can be written as $T = T_0$. Radial and tangential stresses are written as follows:

$$\sigma_r = \frac{F}{r} \tag{7}$$

$$\sigma_r = C_1 r^{k-1} + C_2 r^{-k-1} + A \tag{8}$$

$$\sigma_\theta = \frac{dF}{dr} \tag{9}$$

$$\sigma_\theta = C_1 k r^{k-1} - C_2 k r^{-k-1} + A \tag{10}$$

the integration constants C_1, C_2 and the final term A are determined as follows:

$$A = \frac{(\alpha_r - \alpha_\theta)T_0}{a_{\theta\theta}(1-k^2)} \tag{11}$$

$$C_1 = A\frac{a^{k+1} - b^{k+1}}{b^{2k} - a^{2k}} \tag{12}$$

$$C_2 = A\frac{a^{2k}b^{k+1} - b^{2k}a^{k+1}}{b^{2k} - a^{2k}} \tag{13}$$

Figure 2 shows the disc exposed to thermal stress.

During the analysis, it was assumed that the mechanical properties of composite materials do not change at high temperatures.

3. Findings and discussion

In this study, the distributions of the stress components in the elastic region of three different composite discs consisting of AS4 carbon fiber, T-300 carbon, and $Al_2O_3ZrO_2$ (nanocomposite) were calculated. The disc is fixed, and its dimensions are taken as a = 20 mm, c = 100 mm. Solutions were obtained using temperature values of 45 °C, 60 °C, 75 °C, 90 °C, and 105 °C. The properties of the materials of composite discs are given in **Table 1**[30–32].

Table 1. The stress components of a composite disc with different materials in the elastic region[30–32].

Materials	E_θ	E_r	k	α_r	α_θ	$\upsilon_{\theta r}$
AS4 carbon fiber	235,000	15,000	3.94	-0.5×10^{-6}	15×10^{-6}	0.20
T-300 carbon	230,000	15,000	3.91	-0.7×10^{-6}	12×10^{-6}	0.20
$Al_2O_3ZrO_2$ (nanocomposite)	310,000	310,000	1.00	-12.66×10^{-6}	-12.66×10^{-6}	0.22

The stresses of the discs are given in **Table 2**.

Table 2. The radial stress occurs in the elastic region of the disc.

Temperature ΔT (°C)	Surface	AS4 carbon fiber		T-300 carbon		$Al_2O_3ZrO_2$ (nanocomposite)	
		σt (MPa)	σr (MPa)	σt (MPa)	σr (MPa)	σt (MPa)	σr (MPa)
45 °C	Inner (r = 20)	33.563	0.00	32.849	0.00	44.275	0.00
	Outer (r = 100)	−19.543	0.00	−19.127	0.00	−25.780	0.00
60 °C	Inner (r = 20)	67.126	0.00	65.698	0.00	88.549	0.00
	Outer (r = 100)	−39.086	0.00	−38.254	0.00	−51.560	0.00
75 °C	Inner (r = 20)	100.689	0.00	98.547	0.00	132.824	0.00
	Outer (r = 100)	−58.628	0.00	−57.381	0.00	−77.339	0.00
90 °C	Inner (r = 20)	134.252	0.00	131.396	0.00	177.098	0.00
	Outer (r = 100)	−78.171	0.00	−76.508	0.00	−103.119	0.00
210 °C	Inner (r = 20)	313.255	0.00	306.590	0.00	413.230	0.00
	Outer (r = 100)	−182.399	0.00	−178.518	0.00	−240.611	0.00

In **Figure 3**, the radial stress occurring in the AS4 carbon fiber material disc is given. It can be seen in this figure that for the AS4 carbon fiber disc in 3, the radial stress (r = 46.4 mm) on the inner surface of the disc at 45 °C was 5.44 MPa.

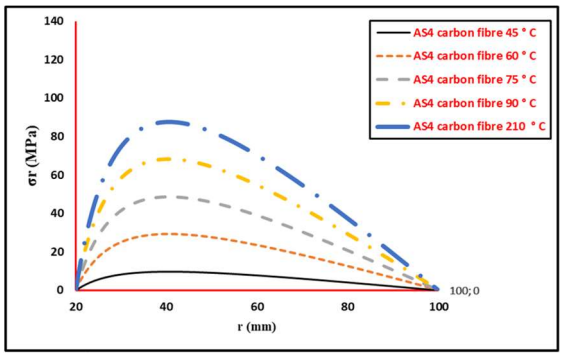

Figure 3. Radial stress occurs in the elastic region of AS4 carbon fiber disc.

It was observed that the radial stress at the innermost part of the disc (r = 46.4 mm) at a temperature of 90 °C was 66.39 MPa. It has been determined that the radial stresses are in the form of compression stress, and the disc has the highest value in the r = 40.8 mm region. Tangential stresses occurring in the elastic region of the AS4 carbon fiber disc are displayed in **Figure 4**.

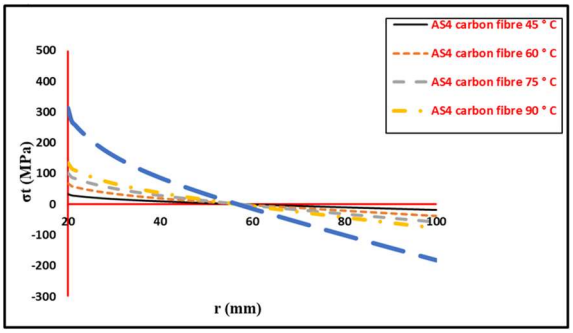

Figure 4. Tangential stress occurs in the elastic region of AS4 carbon fiber disc.

While the tangential stress on the inner surface of the disc at 45 °C was 33.56 MPa, it was observed that the tangential stress in the innermost part of the disc at 90 °C was 134.25 MPa. It has been determined that the tangential stresses are in the form of compression stress up to the region of r = 57.6 mm. From this region of the disc to the outermost part of the r = 100 mm disc, the stresses regularly increase as tensile stress.

In **Figure 5**, the radial stresses occurring in the elastic region of the T-300 carbon disc are displayed.

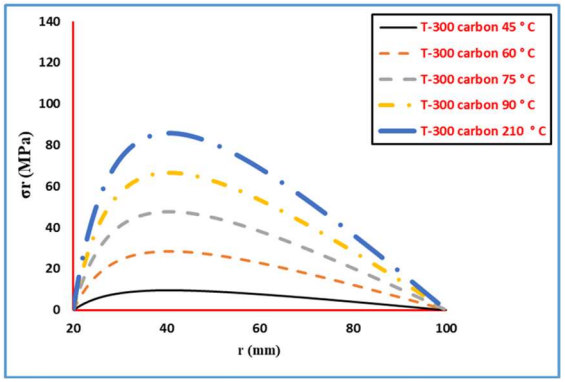

Figure 5. Radial stress occurs in the elastic region of the T-300 carbon disc.

It can be seen in this figure that the radial stress on the inner surface of the disc was at 45 °C (r = 46.4 mm), while it was 9.28 MPa. It was observed that the radial stress at the innermost part of the disc (r = 46.4 mm) at a temperature of 90 °C was 64.98 MPa. It has been determined that the radial stresses are in the form of compression stress, and the disc has the highest value in the r = 40.8 mm region.

In **Figure 6**, the tangential stresses occurring in the elastic region of the T-300 carbon disc are displayed.

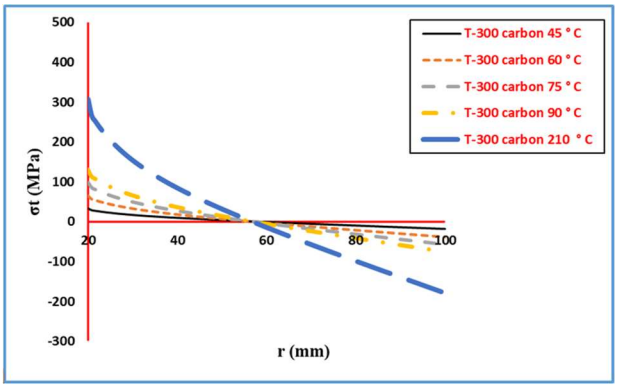

Figure 6. Tangential stress occurs in the elastic region of the T-300 carbon disc.

While the tangential stress on the inner surface of the disc at 45 °C was –32.84 MPa, it was observed that the tangential stress in the innermost part of the disc at 90 °C was 131.39 MPa. It has been determined that the tangential stresses are in the form of compression stress up to the region of r = 57.6 mm. From this region of the disc to the outermost part of the r = 100 mm disc, the stresses regularly increase as tensile stress.

In **Figure 7**, the radial stresses occurring in the elastic region of the $Al_2O_3ZrO_2$ (nanocomposite) disc are displayed.

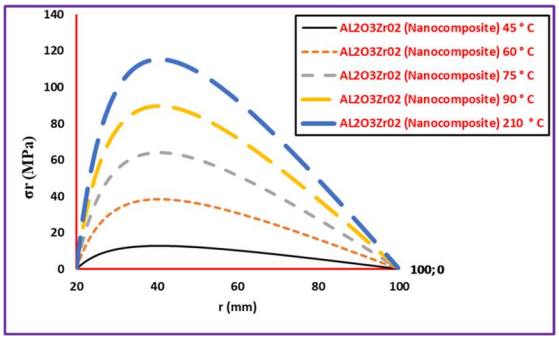

Figure 7. Radial stress occurs in the elastic region of $Al_2O_3ZrO_2$ (nanocomposite) disc.

It can be seen in this figure that the radial stress on the inner surface of the disc was at 45 °C (r = 46.4 mm), while it was 12.51 MPa. It was observed that the radial stress at the innermost part of the disc (r = 46.4 mm) at a temperature of 90 °C was 87.59 MPa. It has been determined that the radial stresses are in the form of compression stress, and the disc has the highest value in the r = 40.8 mm region.

In **Figure 8**, the tangential stresses occurring in the elastic region of the $Al_2O_3ZrO_2$ (nanocomposite) disc are displayed.

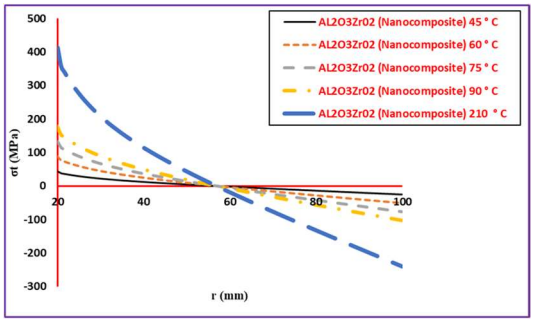

Figure 8. Tangential stress occurs in the elastic region of the $Al_2O_3ZrO_2$ (nanocomposite) disc.

In the case of **Figure 8**, the tangential stresses occurring in the elastic region of the $Al_2O_3ZrO_2$ (nanocomposite) disc are shown. While the tangential stress on the inner surface of the disc at 45 °C was 44.27 MPa, it was observed that the tangential stress in the innermost part of the disc at 90 °C was 177.09 MPa. It has been determined that the tangential stresses are in the form of compression stress up to the region of r = 56.8 mm, and the stresses increase in the case of tensile stress from this region of the disc to the outside. It has been determined that the results of the elastic analysis performed on discs made of different materials are similar to the findings obtained in this study. This is comparable with the literature[18–21]. In **Figure 9** below, the tangential stresses obtained at a temperature of 210 °C are shown in a single graph.

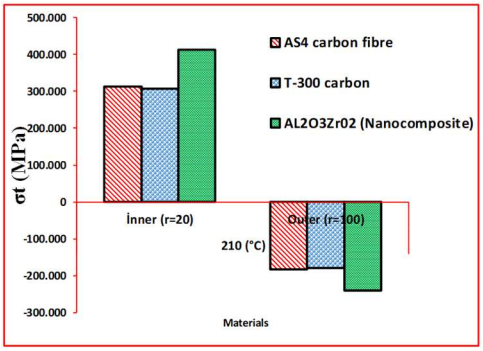

Figure 9. Showing the tangential stresses occurring at a temperature of 210 °C on a single graph.

In their study, Apatay and Eraslan[33] examined the radial and tangential stress and displacement changes that occur in the disc by giving the effect of both mechanical load and thermal load to a rotating disc. According to the results he obtained, the radial stresses are always zero at the innermost and outermost parts of the disc. Tangential stresses, on the other hand, are always greater than radial stresses[33]. As shown in **Figures 3–9**, the radial stresses in the innermost and outermost regions of the discs are always zero in all graphs. The intensity of tangential stress is greater than that of radial stress. The findings obtained coincide with the studies in the literature[34,35]. When the graphs between **Figures 3–9** are examined, it is seen that there are increases in the intensity of radial and tangential stresses with temperature deceleration. This study shows similarities with other studies obtained in the literature[36,37]. The stresses obtained on the disc with $Al_2O_3ZrO_2$ (nanocomposite) material are greater than the stresses calculated on the disc with AS4 carbon fiber material. The stresses obtained on the disc with AS4 carbon fiber material are higher than the stresses obtained on the disc with T-300 carbon material. In other words, the disc with $Al_2O_3ZrO_2$ (nanocomposite) material has the largest stresses. The T-300 carbon disc has the lowest stress. The main reason for this situation is that the mechanical properties of the materials are different. In addition, the modulus of elasticity of $Al_2O_3ZrO_2$ (nanocomposite) material is quite high compared to other materials. The modulus of elasticity is directly related to the stresses that occur. Similarly, in a different study[38], it was found that the stresses obtained in materials with different moduli of elasticity are different from each other.

In **Figure 9**, it is seen that the tangential stress occurring in the $Al_2O_3ZrO_2$ (nanocomposite) disc is higher than in discs with other materials.

4. Conclusion

In this study, elastic thermal stresses were formed by an analytical method. The constant distribution of temperature is taken into account.

Radial and tangential stress components occurring in various temperature distributions from the inner surface to the outer surface of discs consisting of $Al_2O_3ZrO_2$ (nanocomposite), AS4 carbon fiber, and T-300 carbon materials increase with temperature.

It is also clear from this study that if the temperature is constant in each region of the disc, radial stresses occur in the form of compressive stress.

Tangential stresses occur as compression stresses.

The stresses obtained in the disc with $Al_2O_3ZrO_2$ (nanocomposite) material are higher than the stresses obtained in the disc with AS4 carbon fiber material.

The stresses calculated on the AS4 carbon fiber material disc is higher than the stresses calculated on the T-300 carbon disc.

It is high in stresses obtained at very high temperatures. For example, the tangential stress obtained on the inner surface of the $Al_2O_3ZrO_2$ (nanocomposite) disc at 210 °C is 413.22 MPa.

Conflict of interest

The author declares no conflict of interest.

References

1. Ali A, Bayat M, Sahari BB, et al. The effect of ceramic in combinations of two sigmoid functionally graded rotating discs with variable thickness. *Scientific Research and Essays* 2012; 7(25): 2174–2188. doi:

10.5897/SRE11.619
2. Bayat M, Saleem M, Sahari BB, et al. Analysis of functionally graded rotating discs with variable thickness. *Mechanic Research Communications* 2008; 35(5): 283–309. doi: 10.1016/j.mechrescom.2008.02.007
3. Eldeeb AM, Shabana YM, El-Sayed TA, Elsawaf A. A nontraditional method for reducing thermoelastic stresses of variable thickness rotating discs. *Scientific Reports* 2023; 13(1): 13578. doi: 10.1038/s41598-023-39878-w
4. Belhocine A, Bouchetara M. Simulation of fully coupled thermomechanical analysis of disc brake rotor. *Wseas Transactions on Applied and Theoretical Mechanics* 2012; 3(7): 169–181.
5. Ramakrishna S. Mayer J. Wintermantel E, Leong KW. Biomedical applications of polymer-composite materials: A review. *Composites Science and Technology* 2001; 61(9): 1189–1224. doi: 10.1016/S0266-3538(00)00241-4
6. Mouritz AP, Gellert E, Burchill P, Challis K. Review of advanced composite structures for naval ships and submarines. *Composite Structures* 2001; 53(1): 21–42. doi: 10.1016/S0263-8223(00)00175-6
7. Gu GX, Takaffoli M, Buehler MJ. Hierarchically enhanced impact resistance of bioinspired composites. *Advanced Materials* 2017; 29(28): 1700060. doi: 10.1002/adma.201700060
8. Minatto FD, Milak P, De Noni A, et al. Multilayered ceramic composites—A review. *Advances in Applied Ceramics* 2015; 114(3): 127–138. doi: 10.1179/1743676114Y.0000000215
9. Hu T, Zhang Y, Hu L. Mechanical and wear characteristic of Y-TZP/Al_2O_3 nanocomposites. *Industrial Lubrication and Tribology* 2014; 66(2): 209–214. doi: 10.1108/ILT-08-2011-0059
10. Fang Y, Zhang Y, Song J, et al. Design and fabrication of laminated-graded zirconia self-lubricating composites. *Materials & Design* 2013; 49: 421–425. doi: 10.1016/j.matdes.2013.01.040
11. Ghabussi A, Mortazavi M, Betha R. Seismic performance of a cold-formed and hot-rolled steel wall system equipped with curved steel dampers. S*tructures* 2023*;* 53: 296–316. doi: 10.1016/j.istruc.2023.04.053
12. Ghabussi A, Marnani JA, Rohanimanesh MS. Seismic performance assessment of a novel ductile steel braced frame equipped with steel curved damper. *Structures* 2021; 31: 87–97. doi: 10.1016/j.istruc.2021.01.073
13. Nayak P, Saha K. Elastic limit angular speed of solid and annular discs under thermomechanical loading. *International Journal of Engineering, Science and Technology* 2016; 8(2): 30–45. doi: 10.4314/ijest.v8i2.3
14. Lin FW. Elastic analysis for rotating functionally graded annular disc with exponentially-varying profile and properties. *Mathematical Problems in Engineering* 2020; 2020: 2165804. doi: 10.1155/2020/2165804
15. Yildirim V. Thermomechanical characteristics of a functionally graded mounted uniform disc with/without rigid casing. *Journal of Aerospace Technology and Management* 2019; 11: e2919. doi: 10.5028/jatm.v11.1008
16. Peng D, Chen S, Darabi R, et al. Prediction of the bending and out-of-plane loading effects on formability response of the steel sheets. *Archives of Civil and Mechanical Engineering* 2021; 21(2): 74. doi: 10.1007/s43452-021-00227-1
17. Lookpolymers. Hexcel® HexTow™ AS4 carbon fiber. Available online: http://www.lookpolymers.com/polymer_Hexcel-HexTow-AS4-Carbon-Fiber.php (accessed on 17 October 2023).
18. Dragonplate. HexTow® AS4 carbon fiber. Available online: https://dragonplate.com/images/uploaded/pdfs/fiberspecs/as4_hextow_datasheet.pdf (accessed on 17 October 2023).
19. Jelena M, Brcković L, Gajović A. Influence of preparation method and alumina content on crystallization and morphology of porous yttria stabilized zirconia. *Journal of the European Ceramic Society* 2017; 37(9): 3137–3149. doi: 10.1016/j.jeurceramsoc.2017.03.026
20. Sharif AA, Mecartney ML. Superplasticity in cubic yttria stabilized zirconia with 10 wt.% alumina. *Journal of the European Ceramic Society* 2004; 24(7): 2041–2047. doi: 10.1016/S0955-2219(03)00354-6
21. Ai Y, Xie X, He W, et al. Microstructure and properties of $Al_2O_{3(n)}$/ZrO_2 dental ceramics prepared by two-step microwave sintering. *Materials & Design (1980–2015)* 2015; 65: 1021–1027. doi: 10.1016/j.matdes.2014.10.054
22. Özgür TC. *Investigation of the Effect of Different Materials and Constructions on Impact Resistance of Vehicle Bumpers* (Turkish) [Master's thesis]. T. C. Bursa Uludağ Üniversitesi Fen Bilimleri Enstitüsü; 2020.
23. Dashairya L, Chaturvedi V, Kumar A, et al. A benign strategy toward mesoporous carbon coated Sb nanoparticles: A high-performance Li-ion/Na-ion batteries anode. *Solid State Ionics* 2023; 396(1). doi: 10.1016/j.ssi.2023.116243
24. Najmi L, Hu Z. Effects of carbon nanotubes on thermal behavior of epoxy resin composites. *Journal of Composites Science* 2023; 7(8): 313. doi: 10.3390/jcs7080313
25. Najmi L, Zebarjad SM, Janghorban K. Effects of carbon nanotubes on the compressive and flexural strength and microscopic structure of epoxy honeycomb sandwich panels. *Polymer Science, Series B* 2023; 65(2): 220–229. doi: 10.1134/S1560090423700872

26. Sayman O, Duranay M, Gür M, Koçak S. Elastic-plastic stress analysis of a thermoplastic composite disc under uniform temperature distribution. *Science and Engineering of Composite Materials* 2006; 19 (1): 61–77. doi: 10.1515/SECM.2006.13.2.139
27. Dai T, Dai HL. Investigation of mechanical behavior for a rotating FGM circular disc with a variable angular speed. *Journal of Mechanical Science and Technology* 2015; 29(9): 3779–3787. doi: 10.1007/s12206-015-0824-4
28. Çallıoğlu H. Stress analysis of functionally graded isotropic rotating discs. *Advanced Composites Letters* 2008; 17(5). doi: 10.1177/096369350801700501
29. Timoshenko S, Goodier JN. *Theory of Elasticity*. McGraw-Hill; 1970.
30. Drelich J, Tormoen GW. Beach ER. Determination of solid surface tension at the nano-scale using atomic force microscopy. In: Mittal KL (editor). *Contact Angle, Wettability, and Adhesion*. VSP; 2006. Volume 4. pp. 1–28.
31. McCartney LN. Predicting properties of undamaged and damaged carbon fibre reinforced composites. In: Beaumont P, Soutis C, Hodzic A (editors). *The Structural Integrity of Carbon Fiber Composites*. Springer; 2017. doi: 10.1007/978-3-319-46120-5_16
32. Chegg. Available online: https://www.chegg.com/homework-help/questions-and-answers/1-20-fiber-composite-consisted-as4-carbon-fibers-3501-6-epoxy-matrix-engineering-constants-q45618630 (access on 15 September 2023).
33. Apatay T, Eraslan AN. Elastic deformation of rotating discs of parabolic thickness, analytical solutions. *Gazi University Journal of Faculty of Engineering and Architecture* 2003; 18(2): 115–135.
34. Çallıoğlu H, Sayer M, Demir E. Stress analysis of functionally graded discs under mechanical and thermal loads. *Indian Journal of Engineering & Materials Sciences* 2011; 18: 111–118.
35. Sayman O, Yanginci S, Sayer M. Thermoelastic-plastic stress analysis in a thermoplastic composite disc. *Journal of Reinforced Plastics and Composites* 2005; 24(1): 21–33. doi: 10.1177/0731684405041716
36. Leopold WR. Centrifugal and thermal stresses in rotating discs. *Journal of Applied Mechanics* 1984; 15(4): 322–326. doi: 10.1115/1.4009854
37. Manjunath TV, Suresh PM. Structural and thermal analysis of rotor disc of disc brake. *International Journal of Innovative Research in Science*, *Engineering and Technology* 2013; 2(12): 7741–7749.
38. Joshi P, Samantray S, Prabu SS. Investigation on thermal stress analysis of brake disc using ANSYS simulation. *ECS Transactions* 2022; 107(1): 10865. doi 10.1149/10701.10865ecst